WWW.IJRPR.COM

International Journal of Research Publication and Reviews

Journal homepage: www.ijrpr.com ISSN 2582-7421

A Design Approach to the Analysis of Rotor Slip Dominance in Torque Production during Low Slip Motoring

Omogbai Nelson Oyakhilomen [a]; Ogboh Victor C [b].

[a, b]Electrical Engineering Department, Nnamdi Azikiwe University, Awka, Anambra State, Nigeria.
DOI: https://doi.org/10.55248/gengpi.2023.4126

ABSTRACT

The study beams more light on torque production at low slip frequency, where the effect of rotor resistance clearly overrides that of the rotor leakage reactance. It is widely admitted that the cross-sectional area (CSA) of the rotor bar has the major design influence on the rotor resistance (R_2) at this slip region. Besides, the low slip approximation of the developed torque equation tends to reveal that at a given constant voltage and frequency, the only parameter by which the squirrel cage induction motor (SCIM) designer could significantly influence torque development for a given load torque, is the R_2. But it is also widely agreed that torque is operationally dependent on slip, and that the slip at which a given torque is produced rises with R_2 as the slope of the torque speed curve decreases; and this seems to imply the flow of more current at a given operating point. Further, it is also true that this current rise ought to be limited by this increase in R_2 from the design or redesign of the rotor bar. There seems to be a subtle conflict between the individual influence of rotor slip and R_2 as far as torque is concerned. However, this study shows that the superior rate of change of slip, relative to that of R_2 in their respective responses to a design modification in bar CSA, largely supports the fact that slip will always dominate in influence on torque at the high-speed motoring mode of the SCIM.

KEYWORDS: Slip, Rotor resistance, Rotor reactance, Design, Cross sectional area.

1. Introduction

Designing the shape of the rotor bar cross section has a significant impact on the overall performance of the machine. The rotor slot geometry which can be considered as an independent design parameter, is the most influential factor in defining the torque-speed characteristic of the SCIM, especially when mains fed (Di Nardo, Marfoli, Degano, Gerada& Chen, 2020 and Maloma, Muteba& Nicolae, 2017). Lee, Min & Hong, (2013) added that in literature, major focus has been towards finding an optimal design of induction machine geometry with the aim of improving the performance – partly achieved by controlling the resistance and reactance of the rotor circuit, through the design of the rotor bar of the SCIM.

In the low slip motoring region, the rotor frequency is relatively low and the deep bar effect is usually considered negligible (Lipo, 2017). Therefore, with the frequency effects unable to prevail, the entire geometric range of the cross-sectional area of the bar (A) becomes available for the possible realization of an even distribution of both the magnetic flux as well as the full load current (I_{FL}) within the bar section. Hence, the impedances of all parts of the bar are approximately equal and approach their DC values. Though the leakage inductance is higher than during starting and is not significantly affected by factors like skin effect and the saturation of the leakage flux path; but the slip frequency is low, so that for all parallel paths through the bar, it is expected that the bar resistance $R_R$is greater than its leakage reactance X_2 (Chapman, 2005). The mechanical characteristic of an induction motor is linear in the region of small slip frequencies and the value of this slip during normal motor operation determines the running torque (Vukosavic, 2013).

Vukosavic, (2013) explains that with the assumption that the magnetizing current is relatively small, the electromagnetic torque can be shown to be:

$$T_{em} = \frac{3pR_R}{2s\omega_e} \frac{U_s^2}{(R_s + \frac{R_R}{s})^2 + w_e^2(L_{YS} + L_{YR})^2} \quad (1)$$

In equation 1, U_S is the peak value of the phase voltages, p is the number of pole pairs, ω_e is the frequency of stator voltages, and currents. R_s and L_{YS} represent the resistance and leakage inductance of the stator winding respectively. R_R and L_{YR} respectively represent the resistance and leakage inductance of the equivalent two-phase rotor winding that represent the rotor cage and are referred to the stator side. Vukosavic, (2013) went on to emphasize again that if the slip is small, as in when close to rated slip; the rotor speed is close to the synchronous speed. In such a case, impedance $\frac{R_R}{s}$ is the largest of all impedances in the denominator of equation 1. And when only the significant parameters are retained, equation 1 reduces to its small slip approximate form:

$$T_{em} \approx \frac{3spU_S^2}{2R_R\omega_e} \quad (2)$$

Practically, the error in torque determined by equation 2 is less than 2 percent for -0.02 < s < 0.02 [6]. The mechanical characteristic of an induction motor is seen in equation 2 to be linear in the region of small slip frequencies and the value of this slip during normal motor operation determines the running torque (Vukosavic, 2013). Also, beyond the maximum torque as slip drops on the torque-speed curve, developed torque decreases at low slip frequency and increases at high slip frequency (Galindo, Lopez-fdez, Pinto, & Coimbra, 2002). In Guru &Hiziroglu, (2001) some pertinent deductions about equation 2 was made as follows:

a) The torque developed by the motor is proportional to the slip when the applied voltage and rotor resistance are held constant.

b) The torque developed is inversely proportional to the rotor resistance at a given slip when the applied voltage is kept the same.

c) For a constant-torque operation under fixed applied voltage, the motor slip is directly proportional to the rotor resistance. This last point is well buttressed by Lipo, (2017) and Purushothaman, & León, (2011); who empirically showed that under the stated condition, reducing the rotor resistance produces greater slope in the linear region of the torque-speed curve.

This paper attempts to come from the designer's point of view, leveraging on points (a) through (c), and proffer an additional rationale for the established fact that rotor slip governs the level of developed torque at the region of motor operation, close to the synchronous speed.

2. Experimental Set up

The study was conducted at a frequency of 50Hz and 400V L-L with two squirrel cage induction motors (SCIM) – M1(100 HP) and M2 (75HP) which were run in Matlab. Two machines being used here mainly for corroborative purposes. The rotor configurations and specifications of the machines are given in fig 1.

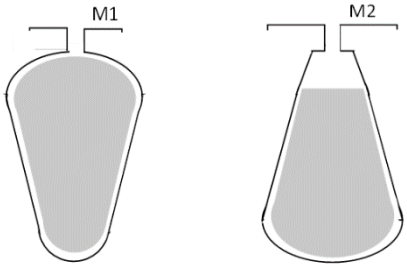

Fig 1: Rotor bar/slot shapes

Table 1: Machine specifications

Paramaters	M1	M2
Number of poles (p)	8	6
Number of rotor slots (Sr)	55	55
Number of stator slots (Ss)	72	72
Full load efficiency (EffR) %	91.12268376	91.0128091
Full load current (I1R) Amps	137.6654083	104.0402237
Full load power factor (PFR)	0.858292383	0.85131468
Full load speed (nmR) rpm	738.5338567	988.106205
Full load torque (TTdR) N.m	972.3504996	545.2107288
Starting Torque (Tst) N.m	1211.62116	1033.85206
Maximum Torque (Tmax) N.m	3368.962837	2406.639801
X1 (ohms)	0.119190885	0.109421793
X2pr (ohms)	0.132792566	0.136917382
Xm (ohms)	3.939174055	4.741771839
R1 (ohms)	0.035604393	0.055371997
R2pr (ohms)	0.042764132	0.049826583
Rc (ohms)	110.5079781	157.5086264

The cross-sectional area (CSA) of the rotor bars of both machines were altered in small incremental steps, and the corresponding effects on the current demand, low slip torque, rotor resistance as well as on the rotor slip were noted.

3. Results and Discussion

For a constant load torque and source voltage, a design intervention to shore up the rotor resistance R_R, is expected to limit current flow and consequently reduce torque production in the linear portion of the torque-slip characteristics in accordance with equation 2, but the M1 and M2 simulation results of fig 2 show noncompliance with this expectation, as the resistance-torque relation seemingly portrayed by equation 2 ought to be: $T_{em}\ \alpha \frac{1}{R_R}$. The proportionality being indicated by α.

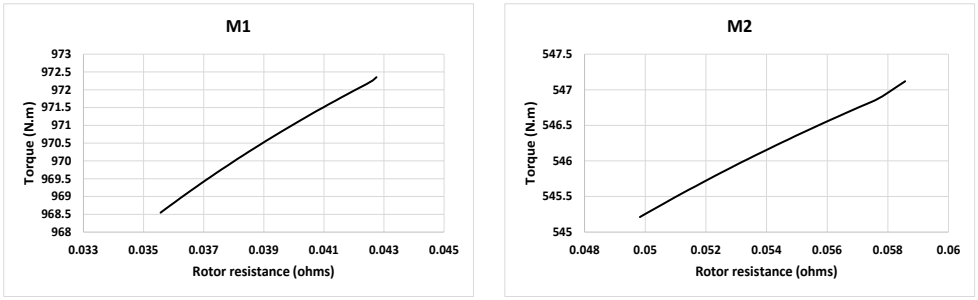

Fig 2: Relation between rotor resistance and small slip torque in the simulated machines

From design perspective, the only significant variables under small slip operating mode in equations 1 and 2 are the rotor resistance ($R_R\ or\ R_2$), and the slip s. R_R is a variable because it could be changed through the modification of the rotor bar CSA (Boldea& Nasar, 2010). Also, besides the fact that the slip is subject to the load torque, the slip associated with a given developed torque is a variable because it is a function of the gradient of the linear portion of the SCIM characteristic. This gradient is in turn largely a function of R_R (i.e., s α R_R) according to authors like Hughes, (2013); Lipo, (2017) as well as Purushothaman, & León, (2011). Chapman, (2005) gave the input current for a phase of the motor from the equivalent circuit of a 3ph SCIM, with all parameters retaining their normal definitions:

$$I_1 = \frac{V_{ph}}{R_1 + jX_1 + \left(\frac{1}{1/R_c + 1/X_m + 1/\left(R_2/s + jX_2\right)}\right)} \qquad (3)$$

The resistance-current relation from machine simulation shown in fig 3 which was run under constant conditions of load torque and of all SCIM parameters except the bar CSA, shows considerable noncompliance with equation 3. This implies that some other variable (the rotor slip) that is dependent on the design modification of the bar CSA is probably behind the observed current trend. Besides, authors like Hughes, (2013) and Cochran, (1989), highlighted that when the rotor slip rises, there is more induced EMF in the rotor, more rotor current flows and thus more torque is produced.

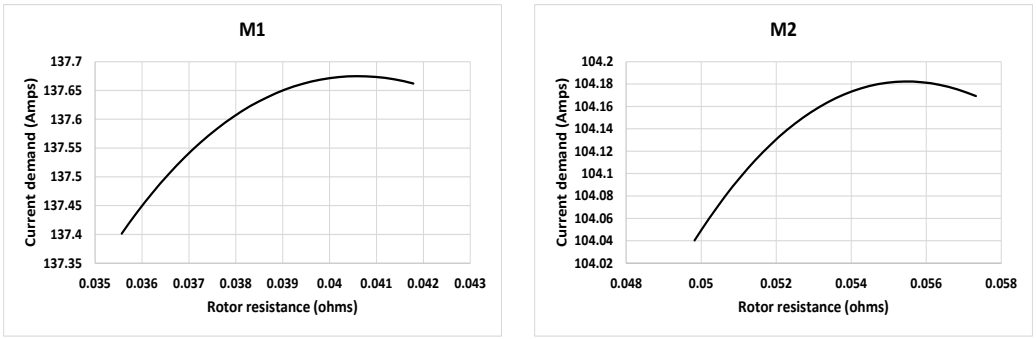

Fig 3: Relation between rotor resistance and current demand in the simulated machines

It is therefore intuitive to deduce that in the small slip operating mode, the slip s governs both equations 2 and 3, as figures 4 and 5 buttress.

Therefore, the designer's torque-centric objective for modifying the CSA of the rotor bar should be to ultimately influence slip through R_R and not necessarily R_R itself; especially in the small slip motor operation. However, the problem still remains unanswered for the SCIM designer, which is: why does R_R appear redundant in equation 2 and seems only significant in conjunction with slip as well as from within the slip?

The answer proffered by this study derives from a simple analysis of the rates of change of both R_R and rotor slip, in their respective responses to instances of a design modification made to the rotor bar CSA. The rotor bar CSA in the case of M1 was changed over a range of 185.6698314 mm^2 to 222.593972 mm^2. While M2 was likewise over a range of 124.6697853 mm^2 to 146.2207148 mm^2. Fig 6 shows the resulting trend.

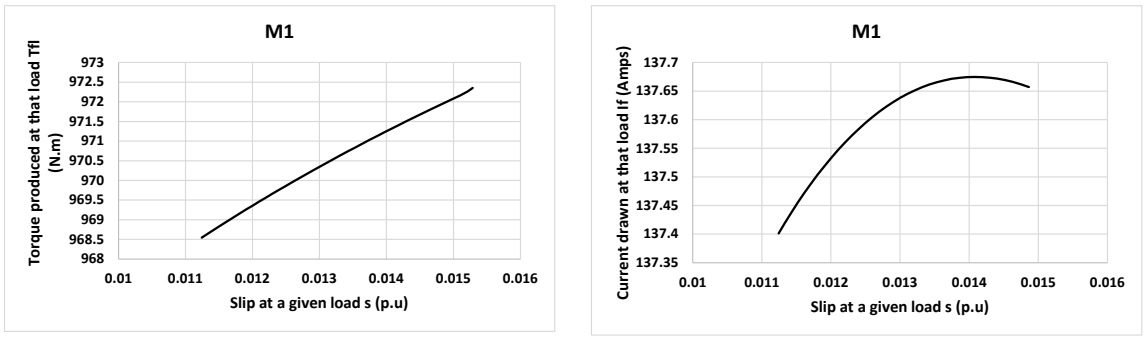

Fig 4: influence of rotor slip on torque and its associated current in machine M1

Fig 5: 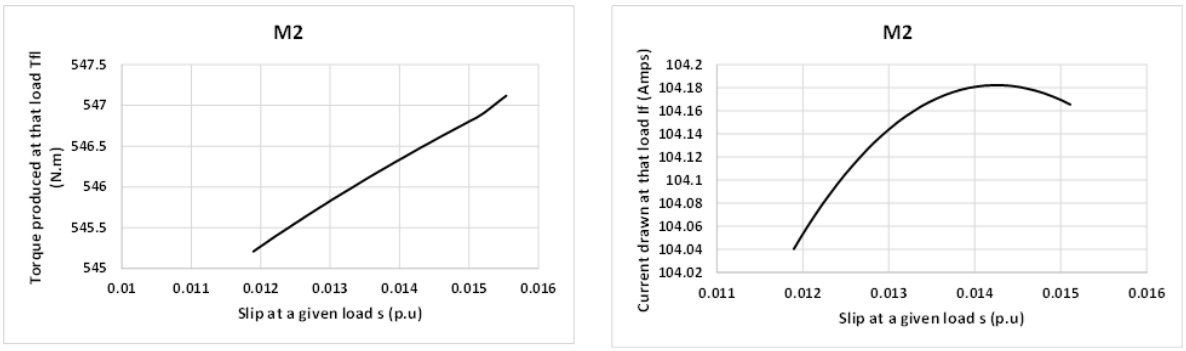

influence of rotor slip on torque and its associated current in machine M2

Mathematicians like Bunday, & Mulholland, (1983) have given the equation of a straight line as:

$$y = mx + c. \quad (4)$$

where, m and c are respectively the gradient and y-intercept of the line.

Comparing equation 4 with the trendline gradients in fig 6 shows that for every step change in the rotor bar CSA, the consequent margin of increase in rotor slip seems to be greater than that observed for the rotor resistance.

Dividing the gradients for each case gives:

for M1: $\frac{trendline\ \ gradient\ \ for\ rotor\ \ slip}{trendline\ \ gradient\ \ for\ rotor\ \ resistance} = \frac{0.0093}{0.0052} = 1.79.$

for M2: $\frac{trendline\ \ gradient\ \ for\ rotor\ \ slip}{trendline\ \ gradient\ \ for\ rotor\ \ resistance} = \frac{0.0078}{0.0045} = 1.73.$

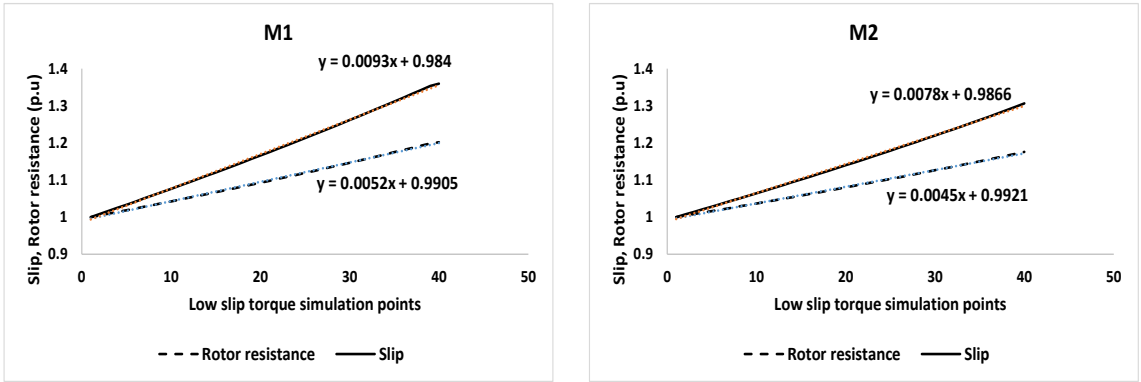

Fig 6: Comparing the respective responses of R_R and slip to design changes in the rotor CSA

Therefore, since at every instance of a design modification of the bar CSA, $\frac{\Delta slip}{slip} > \frac{\Delta R_R}{R_R}$, then the magnitude of the operational impedance $\frac{R_R}{s}$, even after a bar redesign, will definitely be controlled by the slip, which itself is in turn jointly influenced by both bar CSA design and load torque. It may therefore be deduced that the rotor slip, as a remote function of the design variable – the rotor bar CSA; is bound to dominate both equations 2 and 3, as far as small slip torque development is concerned.

4. Conclusion

There now seems to be more evidence to advance the fact that though, the low slip torque is directly proportional to the rotor slip and inversely proportional to the rotor resistance, more light seems to have been shed on the dominance of the rotor slip, in that if the act of rotor bar CSA design/redesign changes the rotor resistance by a factor of x, there is likely to be a resulting change in the gradient of the linear portion of the torque-slip characteristic, and the resulting slip change for a given load torque would be by a factor of approximately 2x; all other variables being held

constant. Therefore, the operational impedance $\frac{R_R}{s}$ at the linear portion of the torque-speed characteristic, upon which torque development rests under the condition of constant source/stator parameters; is unconditionally dependent on the evidently most dynamic parameter – the rotor slip magnitude.

REFERENCES

Di Nardo, M., Marfoli, A., Degano, M., Gerada, C. and Chen, W. (2020). Rotor design optimization of squirrel cage induction motor - part II: results discussion. IEEE. 1 – 9. Doi: 10.1109/TEC.2020.3020263. 30 July, 2021.

Maloma, E., Muteba, M. and Nicolae, D., (2017). Effect of Rotor bar Shape on the Performance of Three Phase Induction Motors with Broken Rotor Bars. 2017 international conference on optimization of electrical an electronic equipment (OPTIM). 364 – 369. Doi:10.1109/OPTIM.2017.7974997.

Lee, G., Min, S. and Hong, J. (2013). Optimal shape design of rotor slot in squirrel-cage induction motor considering torque characteristics. IEEE Transactions on Magnetics. 49 (5), 2197 – 2200, Doi: 10.1109/TMAG.2013.2239626.

Chapman, S. J. (2005). Electric Machinery Fundamentals. Fourth Edition. The McGraw-Hill Companies. Inc. ISBN 0-07- 246523—9, www.mhhe.oom. Pp. 380 =472.

Vukosavic N. S. (2013). Electrical Machines. Springer New York Heidelberg Dordrecht London. ISBN: 978-1-4614-0400-2 (www.springer.com). DOI: 10.1007/978-1-4614- 0400-2. Pp. 365 – 472.

Cathey, J. J. (2001). Electric machines: analysis and design applying Matlab. New York: McGraw-Hill Higher Education. PP. 317 - 420.

Guru B. S. and Hiziroglu H. R. (2001). Electric Machinery and Transformers. New York: Oxford University Press. PP. 509 – 555.

Lipo, T. A. (2017). Introduction to AC Machine Design. New Jersey: IEEE Press, John Wiley & Sons, Inc. PP. 251 – 302.

Purushothaman, S. and León, F. (2011). Eliminating Subsynchronous Oscillations With an Induction Machine Damping Unit (IMDU). IEEE Transactions on Power Systems, Vol. 26, No. 1, Doi: 10.1109/TPWRS.2010.2048438.

Boldea, I. and Nasar, S. A. (2010). The Induction Machine Handbook. Washington, D.C: CRC Press, Taylor & Francis Group. PP. 447 – 473.

Hughes, A., (2013). Electric Motors and Drives: Fundamentals, Types and Applications. 4th edition. Oxford: Newnes.

Cochran, P. L. (1989). Polyphase Induction Motors. Analysis Design and Application. Marcel and Dekker. NY. USA. ISBN 0-8247-8043-4. Pp. 427 – 585.

Bunday, R. D. and Mulholland, H. (1983). Pure Mathematics for Advanced Level. Second edition. Butterworth & Co Ltd. Great Britain.

Galindo, V. A., Lopez-fdez, X. M., Pinto, J. A. D. and Coimbra, A. P. (2002). Parametric Study of Rotor Slot Shape on a Cage Induction Motor. Studies on Applied Electromagnetics and Mechanics. 190 – 195. Vol 22. Retrieved from www.google.com. 17 September, 2021.